ORIGINAL PAPER

Novel Bio-based Immiscible Blends of Poly(Butylene Succinate)/Poly(Ethylene Brassylate): Effect of PEB Loading on Their Rheological, Morphological, Thermal and Mechanical Properties

Wendy Sartillo-Bernal[1] · Roberto Yáñez-Macías[1] · Ricardo López-González[1] · Jesús Francisco Lara-Sánchez[1] · Javier Gudiño-Rivera[1] · Heidi Andrea Fonseca-Florido[2]

Abstract

Poly(butylene succinate) (PBS)/poly(ethylene brassylate) (PEB) biodegradable polyester blends were prepared at different PEB contents (5 to 30 wt%) to study the influence of the addition of PEB on the rheological behavior, morphology, thermal and mechanical properties of the blends. A gradual decrease in the shear viscosities and a greater shear thinning behavior were observed with increasing PEB content due to its low molecular weight, which acted as a lubricant or plasticizer, favoring the disentanglement of PBS chains. The blends with higher PEB content (25 and 30 wt%) had higher activation energy values and were more sensitive to temperature variations. The morphology showed good dispersion of PEB in the PBS matrix. Still, increased PEB content led to larger droplets, indicating immiscibility and poor adhesion between phases. PEB influenced both nucleation density and spherulite size of PBS/PEB blends, denoted by an increasing degree of crystallinity, a shift to low crystallization temperatures, and an improvement in the decomposition temperature according to their thermal properties. Low PEB contents (5 and 10%) increased PBS toughness due to the higher crystalline fraction and smaller crystal size of these blends.

Keywords Poly(Ethylene Brassylate) · Biodegradable Blends · Morphology · Rheology · Thermal Properties

Introduction

The demand for environmentally friendly alternatives has promoted the development of bio-based and/or biodegradable polymers at the academic and industry research level, increasing their different applications, e.g., automotive, textile, packaging, and medical sectors. Polymer blends have been an important strategy to promote the use of biodegradable polymers because its practical and lower cost than other approaches (reactive compatibilization, nanocomposites, complex synthesis techniques, etc.) [1] and feasible to scale up using conventional plastics processing equipment (extrusion, injection molding, blowing, thermoforming, etc.). Depending on the intrinsic characteristics of the polymers, ratio, mixing method, and the use or not of compatibilizing agent, blends can be classified into miscible (homogeneous morphology) and immiscible (phase separation), the latter being more common [2], both are intimately related with the properties like crystallinity, melt strength, thermal stability, rheology, which impact the processing and final properties [3].

Polybutylene succinate (PBS) is an aliphatic biodegradable polyester that is soft, flexible, and semicrystalline. It has exceptional melt processability, thermoplastic behavior, chemical resistance, and much higher ductility than other biodegradable polymers (PLA and PHA). However, PBS has low thermal stability and poor mechanical properties [2, 4, 5]. More extensive research and development have

✉ Javier Gudiño-Rivera
javier.gudino@ciqa.edu.mx

✉ Heidi Andrea Fonseca-Florido
heidi.fonseca@ciqa.edu.mx

1 Centro de Investigación en Química Aplicada (CIQA), Blvd. Enrique Reyna H. No. 140, Saltillo, Coahuila C.P 25294, México

2 Centro de Investigación en Química Aplicada (CIQA), Investigador por México-CONAHCYT, Blvd. Enrique Reyna H. No. 140,, Saltillo , Coahuila C.P 25294, México

been undertaken in biodegradable blends of PBS with polymers like polylactic acid (PLA) [6], polyhydroxybutyrate (PHB) [7], poly(butylene adipate-*co*-terephthalate) (PBAT) [8], polycaprolactone (PCL) [9], and thermoplastic starch-based blends [10]. But more recently, the synthesis of new biodegradable polymers has been reported, as is the case of polyethylene brassylate (PEB), a polyester synthesized by ring-opening polymerization of ethylene brassylate. PEB is easily susceptible to hydrolytic degradation, and ethylene brassylate is commercially large-scale and low-cost. It is also used in many fragrances because of its sweet, musk-like odor. PEB and PCL have similar properties, like melting temperatures around 60–70 °C but higher glass transition temperatures of -30 °C and − 60 °C, respectively [11–13]. The addition and effect of PEB in polymeric blends have not been reported.

The changes in the properties of polymeric PBS blends have been studied. For example, in PLA/PBS blends, Budtri et al. [14] found a decrease in the melting temperature, the tensile strength, and Young's modulus but an increase in elongation at break and phase separation of a higher proportion of PBS. Barletta et al. [15] produced a low-cost bioplastic material from PLA/PBS blends that can be thermoformed, designed explicitly for polyolefins. Adding calcium carbonate to the blends induced crystallization and yielded a stiffer material. Due to PLA's higher viscosity, it presents a hindered droplet breakup mechanism of the PLA phase in the PBS matrix, and hence, a viscosity ratio stays > 1 of PLA/PBS related with heterogeneous blend morphologies with coexisting droplets of the minor phases for different blend compositions [16]. Otherwise, Barletta et al. [15] noticed that in membranes formulated with biodegradable PCL/PBS blends, PBS content above 20 wt% increased the membrane porosity and decreased the mechanical properties, but higher PBS concentration decreased porosity and increased the tensile properties. In another study, PHB (Polyhydroxybutyrate)/PBS immiscible blends were obtained by melt mixing without the addition of compatibilizers. The authors observed variations in blend morphologies (co-continuous or matrix-droplets), a droplet's size increasing according to the proportion of the blend, and an improvement in ductility as the PBS content increased [17]. According to the literature, polymer blends allow design characteristics suitable for different processing equipment depending on the desired application and diminish costs, processing times, and improvements during processing (low viscosity, higher thermostability, and faster crystallization rate).

This work aims to report, for the first time, a novel blend of PBS with PEB, a high crystalline polymer with low molecular weight, low crystallization, and melting temperature. Due to the thermoplasticity of both polymers and their biodegradability, this blend has potential applications in 3D

and 4D printing filament for biomedical devices [18], and tissue engineering scaffolds [19]. After, an in-depth rheological analysis was performed to understand further the effect of PEB content and temperature on the shear viscosity of the PBS/PEB blends using the Cross model and the Arrhenius equation. Understanding the rheological properties of biodegradable polymer blends is necessary to improve their thermal processing conditions and potential use without producing extensive thermal degradation during a specific residence time due to the sensitivity of their viscosities to the effect of shear rate and temperature. The impact of PEB content on the morphology, crystallinity, thermal and mechanical properties of PBS/PEB blends was studied.

Experimental Section

Materials

The polybutylene succinate (BioPBS FZ71PM) (injection molding grade, melt index: 22 g/10 min at 190 ºC, 2.16 kg, and density: 1.26 g/cm^3) was obtained from PTT MCC Biochem Company Limited. The molecular weight of BioPBS was reported to range from 100,000 to 150,000 Da [2, 20]. Ethylene brassylate monomer (> 97% purity) was purchased from Ventos S.A. Toluene was supplied by Baker (reactive grade). 1,5,7-triazabicyclo [4,4,0] dec-5-en (TBD) was purchased from TCI Chemical, and the benzyl alcohol was acquired from Sigma Aldrich (> 98% purity), which acted as an initiator, was also obtained from Sigma Aldrich.

Synthesis of the Polyethylene Brassylate (PEB)

Poly (ethylene brassylate) homopolymer was synthesized in a 1 L stainless steel Delta Reactory reactor equipped with a turbine-type mechanical stirrer. Heating was provided with electrical resistance and cooling was with cold water flowing through an internal tubing coil. The reaction was carried in toluene solution at 90 °C by 8 h, and a speed agitation of 400 rpm. Toluene (380 mL), and the ethylene brassylate monomer (333 mL, 1.6733 mol) were added at the reactor at atmospheric conditions to obtain a ratio monomer/solvent 50/50% w/w (considering too the toluene used in the initiator system solution). The reactor was closed, heated, and stirred to reach the reaction temperature.

Separately, the initiation system 1,5,7-triazabicyclo[4.4.0]dec-5-ene (TBD)/benzyl alcohol (BAc) in solution was prepared inside an MBrown glove box. The TBD/BAc was dissolved in toluene in 30 ml glass containers equipped with magnetic stirrers and sealed with rubber septa. In the glass containers, 2.9106 g (0.2091 mol) of TBD crystals were weighed and closed with rubber septa, and 20
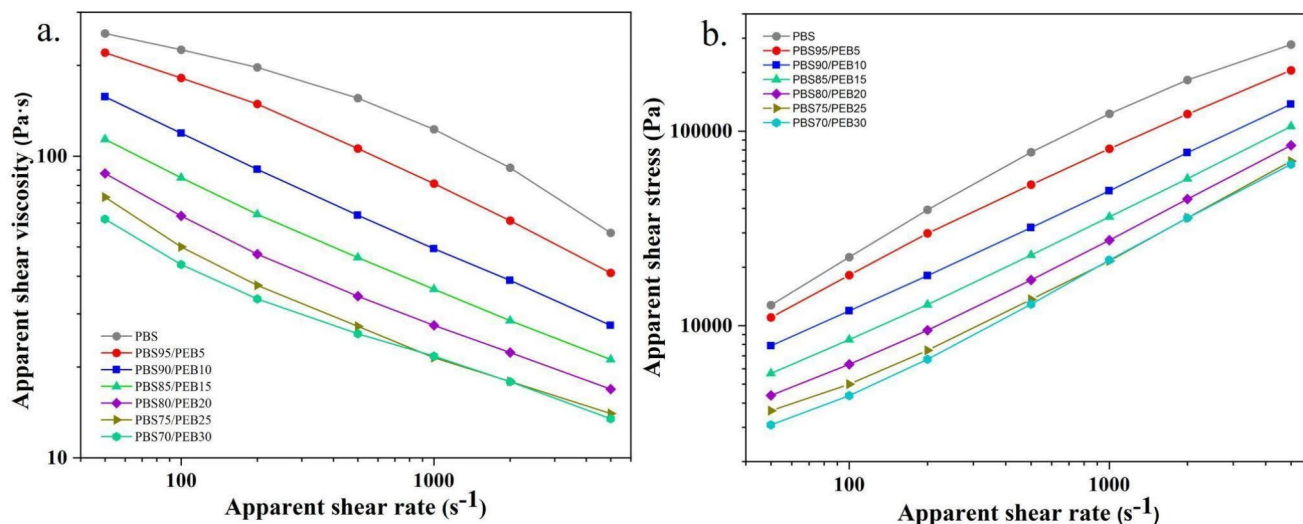
Fig. 1 Capillary rheometry of PBS/PEB blends at 130 °C: (a) shear viscosity curves, (b) shear stress curves
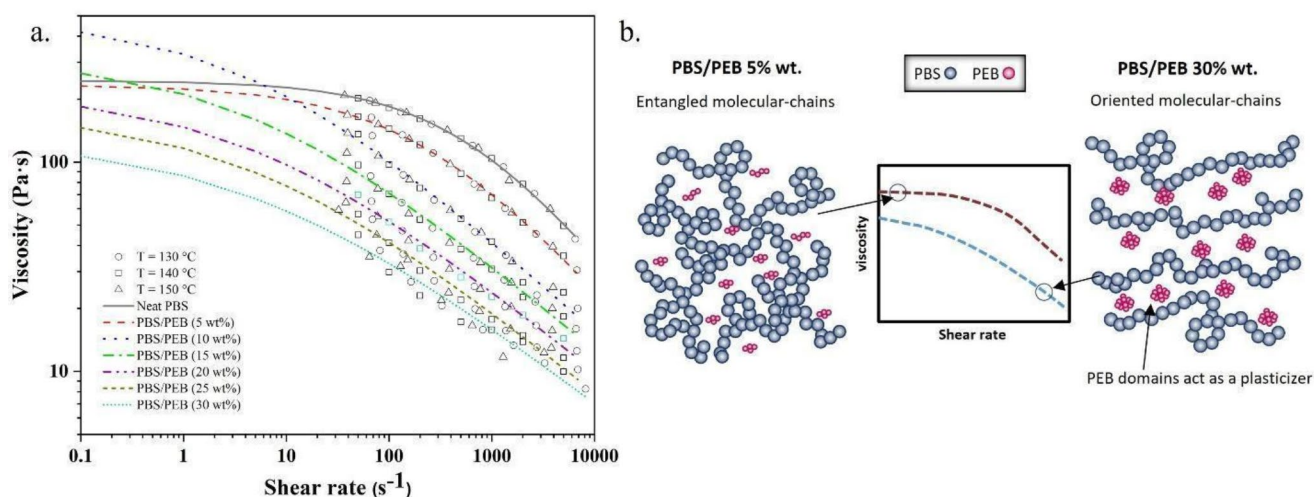

Fig. 2 (a) Shear viscosity master curves of neat PBS and PBS/PEB blends at a reference temperature of 140 °C. (b) Representation of entanglement and disentanglement of PBS chains according to shear rate and PEB content

mL of toluene and 0.43 mL (0.00418 mol) of BAc were subsequently added with syringes. The containers were stirred to complete TBD dissolution.

Once the reactor reached the reaction temperature and the initiator solution was completely dissolved, the latter was added to the reactor using a syringe, and the reaction proceeded under the conditions described above. At the end of the reaction time, the mixture was poured over cold methanol to precipitate the PEB and finally filtered and dried to constant weight in a vacuum oven at 60 °C and 30 mm Hg pressure. The PEB was characterized by gel permeation chromatography (GPC) (see supplementary information Fig. 1S) and proton nuclear magnetic resonance (^{1}H NMR) (Fig. 2S). The molecular weight (Mw = 18400 Da)

and dispersity (D = 2.42) of PEB were determined by GPC (Table 1S).

Preparation of PBS/PEB Blends

Blends of PBS/PEB were prepared by melt mixing for 10 min in a Banbury chamber (Brabender, ATR model) with roller rotors at 130 ºC and 80 rpm. The ratios of PBS and PEB by weight were: PBS100/PEB0, PBS95/PEB5, PBS90/PEB10, PBS85/PEB15, PBS80/PEB20, PBS75/PEB25 and PBS70/PEB30. After melt mixing, thick plates (1 mm) were obtained by compression molding using two hydraulic presses (PHI, model Q230H-X4A, United States) for heating and cooling at 130 ºC and 25 ºC, respectively.

Table 1 Cross-arrhenius model parameters and activation energy of neat PBS and PBS/PEB blends ($T_0 = 140$ °C)

Sample	Neat PBS	5%	10%	15%	20%	25%	30%
η_o (Pa·s)	240.89	236.84	498.95	316.94	221.65	175.55	106.89
τ^* (Pa)	142492.44	52171.96	2389.89	1677.75	1241.66	984.56	725.29
m (-)	0.628	0.568	0.448	0.421	0.408	0.407	0.367
r^2 (Cross)	0.999	0.999	0.992	0.989	0.987	0.984	0.948
a_T (130 °C)	1.333	1.319	1.326	1.314	1.330	1.354	1.608
a_T (140 °C)	1.000	1.000	1.000	1.000	1.000	1.000	1.000
a_T (150 °C)	0.761	0.768	0.764	0.771	0.762	0.749	0.636
r^2 (Arrhenius)	0.998	0.998	0.995	0.999	0.999	0.999	0.999
Ea (kJ/mol)	39.77	38.31	39.05	37.83	39.50	42.01	65.83

Capillary Shear Rheology

Rheological measurements were carried out at different temperatures and shear rates on a high-pressure capillary rheometer (Rheograph 25, Goettfert) with a barrel diameter of 15 mm and a die with an L/D ratio of 30:1. Before any measurement, the samples were dried in a vacuum oven for 12 h to eliminate humidity. The specimens were evaluated in a wide shear rate range of 50 to 5,000 s^{-1}, suitable for different plastic processes such as extrusion and injection molding. The tests were carried out at temperatures above the melting point of PBS and PBE (see Table 1), which are 130, 140, and 150 °C. The data were analyzed using the Cross-Arrhenius model to obtain the master curves at a reference temperature of 140 °C.

Morphological Properties

The morphological structure of the samples was analyzed using a scanning electron microscope (SEM) (JCM600, JEOL). The cryogenic fracture was done with liquid nitrogen. All samples were coated with gold–palladium to ensure their conductivity and placed on double-sided copper tape. The voltage used was 10 kV. The particle size of the dispersed phase was obtained by measuring twenty particles and processed with the ImageJ software for each blend. The spherulite morphology was analyzed using a polarizing optical microscope (POM, BX51, Olympus). The PBS/PEB blends were heated from room temperature to 150 °C and kept for 5 min. Then, the blends were cooled to 40 °C at 10 °C/min. Q-capture pro 7 software was used to calculate the size of the PBS spherulites.

X-ray Diffraction (XRD)

The X-ray diffraction patterns were obtained in a diffractometer (D8 Advance Eco, Brucker) ranging from 5° to 80° at 2θ with an intensity of 25 mA and a voltage of 40 kV. The crystalline fraction ($X_{C, XRD}$) of the polymer was based on estimating the area under the curve of the crystalline peaks

(A_c) and the amorphous area (A_a) of each sample using the Origin Pro 9.0 software (version 9.0). The Eq. (1) was used.

$$X_{c,XRD} = \frac{A_c}{A_a + A_c} \tag{1}$$

Thermal Properties

To establish the thermal stability of each sample, a thermogravimetric analyzer (TGA, Q500 TA Instruments) was employed. The TGA was evaluated in a heating ramp of 10 °C/min in a nitrogen atmosphere at a temperature range from 25 to 600 °C, and then it was changed to oxygen until 800 °C.

The evaluation of thermal properties was done by differential scanning calorimetry (DSC) (2500, TA Instruments Discovery series). About 5 to 7 mg were encapsulated in a DSC aluminum pan. First, the specimen was heated from 0 to 130 ºC, at a heating rate of 10 ºC/min, and kept for 3 min to eliminate the thermal history. Then, the sample was cooled to room temperature at a cooling rate of 10 °C/min. Finally, it was reheated to 130 °C at a heating rate of 10 °C/min. The crystalline fraction from first melting ($X_{c1, DSC}$) and second melting ($X_{c2, DSC}$) was calculated according to the Eq. (2) where $\Delta H°_m$ is the enthalpy of fusion of the totally crystalline (100% crystalline) specimen, $\Delta H°_m = 110.3$ J/g, and ω represents the weight fraction of PBS in the blends [21].

$$X_{c,DSC} = \frac{\Delta H_m}{w \times \Delta H°_m} \times 100 \tag{2}$$

Mechanical Properties

The tensile properties as Young's modulus (E), the tensile strength (σ), and the elongation at break (ε) were evaluated by a stress-strain test on a universal machine (model 43, MTS Advantage™), a cross-head speed of 5 mm/min, with a 100 Lb load cell and a grip separation of 1 according to

the ASTM D-638 standard. Five replicates were tested for each sample.

Statistical Analysis

Statistical analyses (ANOVA) were carried out with Tukey's statistical test homogenous groups ($p \leq 0.05$) using the Origin software system (version 2022b).

Results and Discussion

Flow Behavior of PBS/PEB Blends

The effect of PEB content on the viscosity of its blends with PBS was evaluated by capillary rheometry at different shear rates and temperatures. Capillary rheometry is a more suitable technique for assessing the shear viscosity of materials used in processes such as injection molding and additive manufacturing (AM) because the materials can be subjected to higher pressures and, therefore, at intermediate to high shear rates.

Neat PBS and its blends with PEB exhibited a pseudoplastic behavior; the apparent shear viscosity decreased with an increasing shear rate (Fig. 1a), and the apparent shear stress increased with an increasing shear rate (Fig. 1b), which was produced by molecular chain disentanglement due to the rising force applied to the material to flow [22, 23]. Moreover, a gradual decrease in the melt viscosities of the blends, shear stresses, and a more pronounced shear thinning behavior was observed with increasing PEB content, indicating that the low molecular weight molecules of PEB had a lubricant effect on the PBS matrix enhancing the movement of molecular chains and chain slippage [24]. These curves were also obtained at 140 and 150 °C to construct the master curves (see supplementary information, Fig. 3S).

Rheological models describe the dependence of shear viscosity (η) on shear rate (γ) and temperature (T). The analysis of the shear viscosity data obtained at different shear rates was carried out using the Cross model represented by the following equation [25].

$$\eta = \frac{\eta_0}{1 + \left(\frac{\eta_0 \gamma}{\tau *}\right)^m} \tag{3}$$

Where η_0 is the zero shear viscosity, the viscosity plateaus as the shear rate approaches zero, $\tau*$ is the critical shear stress, and m is the viscosity exponent (m = 1 - n). This model was selected because it combines the Newtonian and the power law shear thinning regions observed in the PBS apparent viscosity curve (see Fig. 2a).

The dependence of shear viscosity on temperature can be modeled using two different mechanisms considering the material processed and the temperature range [26]. For T_g < T < T_g + 100 °C, where T_g is the glass transition temperature of the polymer, the William-Landel-Ferry (WLF) model describes the temperature effect. This model considers the free volume available for molecular motions and better describes the temperature dependence of the viscosity of amorphous polymers. For T > T_g + 100 °C, the free volume is not a limiting factor, and the temperature dependence follows an Arrhenius-like equation. It is suitable to describe the temperature dependence of the viscosity of thermoplastic polymers [27].

According to these criteria, the Arrhenius model could adequately describe the temperature dependence of the shear viscosity of the neat PBS, PEB, and its blends because the test temperatures selected for this analysis were 130, 140, and 150 °C. The T_g of PBS was − 34.11 °C, and for PEB, it was − 31.14 °C.

The Tg for neat PBS, neat PEB, and their blends were obtained by DSC using a heating ramp of 20 °C/min (see Fig. 4S and Table 2S in the supplementary information). The relationship of a polymer blend's Tg with its composition reflects miscibility or lack thereof [28]. PBS and PEB had Tg values close to each other, and their blends had a single Tg. Still, their values did not have a relationship with
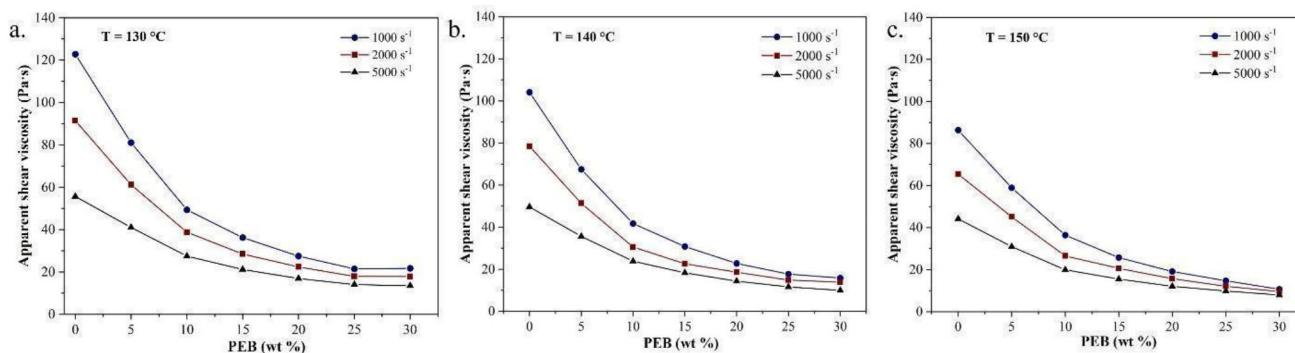

Fig. 3 Effect of shear rate on the apparent shear viscosity of PBS/PEB blends at different temperatures: (a) 130 °C, (b) 140 °C and (c) 150 °C

Fig. 4 Morphology of PBS/PEB blends observed by SEM. Numbers represent the average size of the dispersed phase (different lowercase letters indicate a significant difference ($p \leq 0.05$))
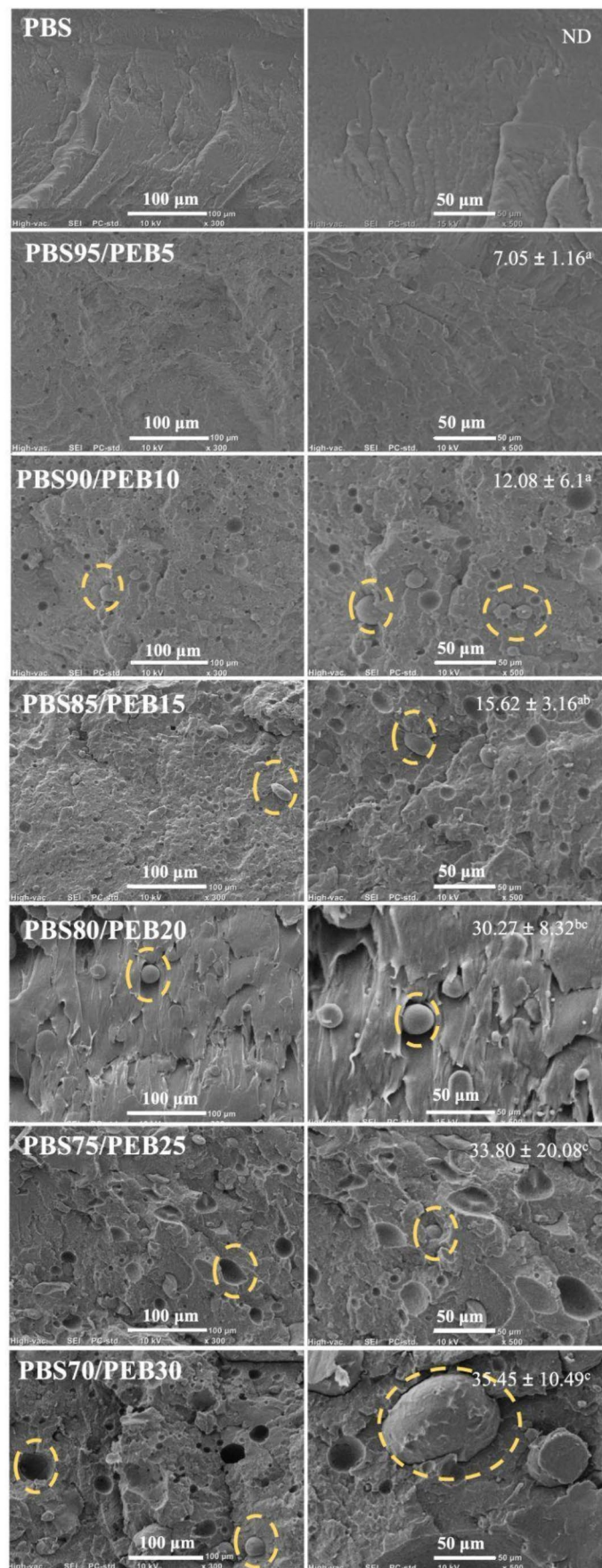
Table 2 Parameters of DSC during crystallization and melting stage and percentage of crystallinity

Samples/stage	Crystallization				Melting (2nd heating)						$X_{C2,DSC}$	X_{CXRD}
	PEB		PBS		PEB		PBS					
	Tc (°C)	ΔHc (J/g)	Tc (°C)	ΔHc (J/g)	Tm (°C)	ΔHm (J/g)	Tcc (°C)	ΔHcc (J/g)	Tm (°C)	ΔHm (J/g)	(%)	(%)
PBS	-	-	64.92±0.1	51.17±0.1	-	-	95.19±0.4	7.69±0.4	115.07±0.9	50.79±0.6	46.05±0.37	39.00±0.5[e]
PBS95/PEB5	46.23±0.2	3.94±0.1	78.16±0.3	69.02±0.6	69.56±0.8	3.2±0.4	100.1±0.2	8.24±0.8	114.63±0.9	69.75±0.1	66.56±0.45	47.90±0.2[d]
PBS90/PEB10	48.01±0.9	7.87±0.4	75.88±0.7	64.15±0.7	69.15±0.5	7.34±0.6	98.39±0.1	9.25±0.4	114.44±0.9	67.15±0.7	67.64±0.62	43.3±0.3[c]
PBS85/PEB15	48.76±0.9	12.5±0.8	73.38±0.9	59.18±0.9	69.7±0.2	9.14±0.9	97.32±0.7	8.74±0.7	114.99±1.2	65.25±0.7	69.60±0.58	40.8±0.2[be]
PBS80/PEB20	50.85±0.5	16.47±0.2	76.78±0.5	59.19±0.6	69.6±0.7	12.65±0.6	99.01±0.4	7.78±0.6	114.73±0.9	62.32±0.2	70.64±0.93	40.6±0.6[be]
PBS75/PEB25	51.81±0.4	17.5±0.2	75.15±0.4	52.2±0.4	69.71±0.5	17.09±0.3	98.44±0.3	7.81±0.2	114.59±0.3	54.94±0.9	66.46±0.86	41.1±1.0[b]
PBS70/PEB30	54.21±0.3	21.91±0.1	74.45±0.5	48.9±0.3	69.85±0.2	22.18±0.9	98.21±0.6	7.5±0.8	114.84±0.6	52.01±0.4	67.36±0.21[b]	42.4±0.6[bc]
PEB	52.37±0.9	109.11±1.0	-	-	69.78±0.4	101.77±0.4	-	-	-	-	-	56.3±0.8[a]

the composition, indicating that these blends were immiscible, as was confirmed by the morphology analysis by SEM (see Fig. 4).

To construct the viscosity master curves, the shear viscosity curves obtained at different temperatures were superposed by applying the time-temperature superposition principle (TTS) using the Arrhenius shift factor (a_T) of the following equation [29].

$$aT = \frac{\eta_0(T)}{\eta_0(T_0)} = exp\left[\frac{E_a}{R}\left(\frac{1}{T} - \frac{1}{T_0}\right)\right] \qquad (4)$$

Where Ea is the activation energy (J/mol) at the reference temperature T_0 (K), and R is the ideal gas constant (8.314 J/mol·K). The shift factors, activation energy, and parameters of the Cross-Arrhenius model were calculated using Goettfert's WinRheo software and were listed in Table 1.

Figure 2a shows the master shear viscosity curves for neat PBS compared with its blends with PEB at a reference temperature of 140 °C. The master curves of neat PBS and PBS95/PEB5 revealed a Newtonian plateau in a wide range of shear rates and a transition zone before the pseudoplastic region. Incorporating 5 wt% of PEB reduced the shear viscosity values but produced a similar rheological behavior compared with neat PBS. Adding 10 to 30 wt% of PEB significantly changed the rheological behavior of PBS; the shear viscosity curves displayed only the transition to the pseudoplastic region without the Newtonian plateau. Gui et al. [30] reported a similar behavior in poly (lactic acid)/ poly (butylene succinate adipate) blends. PLA/PBSA blends had pronounced shear thinning behavior and did not show a Newtonian plateau like the pure components. This rheological behavior was attributed to an increased sensitivity of the melt blend to shear flow due to the deformation of the dispersed phases. Figure 2b illustrates, at low PEB content and low shear rate, PBS chains showed entanglement and hence higher viscosity; on the contrary, an increase of PEB content and higher shear rate, gave rise to more domains or droplets of PEB (as shown in SEM, Fig. 4) and hence, PBS molecular chains exhibited higher orientation which reduced the viscosity of blend.

The zero-shear viscosity decreased in the PBS95/PEB5 but then increased in the PBS90/PEB10 due to the change in the above-mentioned rheological behavior. Walha et al. [31] attributed the higher viscosity of a relatively low molecular weight PA11 in immiscible blends with PLA to the higher polydispersity and intermolecular interactions between the macromolecular chains and a corresponding effect in its rheological behavior. Then, the blend's viscosity gradually decreased when the PEB content rose to 30 wt% due to the low molecular weight of PEB. Another observed change in the parameters was the gradual decrease in the

viscosity exponent (m), which indicated a higher effect of the shear rate on the viscosity with PEB content. The activation energy for the viscous flow of Eq. 3 was valid for temperatures at least 100 K, above the glass transition temperature, and it reflected the temperature sensitivity of the shear viscosity [32]. The blends' activation energy values (see Table 1) remained stable up to 20 wt% PEB content. The high activation energy values of PBS75/PEB25 and PBS70/PEB30 indicated that their shear viscosities were more sensitive to temperature, due to the higher content of low-molecular-weight PEB molecules.

Effect of PEB Content on the Shear Viscosity of PBS/PEB Blends

The shear viscosity of polymer blends was influenced by the average molecular weight and concentration of its components. Figure 3 shows the relationship between the apparent shear viscosity on PEB content at different temperatures (130, 140, and 150 °C) and shear rates (1000, 2000, and 5000 s^{-1}). A non-linear decrease in the blend's apparent shear viscosity with increasing PEB content was observed. Moreover, it was notable that the shear viscosity decreased with the increase in temperature, shear rate, and PEB content. A PEB content of 10 wt% decreased the viscosity of neat PBS by 60% at 130 °C, and similar changes were observed at 140 and 150 °C. The shear viscosity dropped at higher contents, but the change was lower. In some applications, like injection molding, the structures need to be manufactured with thin wall thicknesses, requiring materials with low viscosity to fill the cavities without relying on high temperatures, which result in material degradation. This aspect is critical when using biodegradable polymers because their thermal stability is lower than non-biodegradable synthetic polymers. PEB content at 5 wt% considerably reduced neat PBS's shear viscosity (approximately 34%) without modifying its rheological behavior and thermal stability (see the activation energy values in Table 1).

Effect of Temperature on PBS/PEB Blends

Temperature significantly affects the shear viscosity of polymers, and for semicrystalline linear homopolymers at temperatures above their melting point, this dependence is represented by an Arrhenius-like equation [33].

$$\eta\left(T\right) = \kappa_0 \bullet exp\left(\frac{E_a}{RT}\right) \quad (5)$$

Where η is the shear viscosity, k_0 is the pre-exponential factor, E_a is the flow activation energy, T is the absolute temperature, and R is the ideal gas constant. This equation can be expressed in another form by taking the logarithm of both sides.

$$In\left(\eta\right) = \left(\frac{E_a}{R}\right)\left(\frac{1}{T}\right) + In\left(\kappa_0\right) \quad (6)$$

Thus, the flow activation energy values were calculated from the slopes of the graph of ln η vs. 1/T (see supplementary information, Fig. 5S) for the higher shear rate analyzed (5000 s^{-1}) and different PEB contents. The activation energy values and its correlation coefficients (r^2) are listed in Table 3 S (see supplementary information). The shear viscosity exhibited a linear increase with the reciprocal of absolute temperature and decreases with increasing the PEB content at a constant shear rate of 5000 s^{-1}. It was seen that the slope of the lines (E_a/R) gradually remained almost constant with PEB loading until a maximum of 25%. These results agree with the Ea values calculated with the Cross-Arrhenius model (see Table 1). The blend (PBS70/PEB30) with a higher flow activation energy was more sensitive to variations in the temperature due to the higher content of low molecular weight PEB. Generally, an increase in the melting temperature is used to reduce the viscosity of the melt during injection molding. However, biodegradable polymers are not as suitable due to their low thermal stability. Thus, blending biodegradable polymers with low molecular weight polymers, such as PEB, may be a more effective alternative to reduce the viscosity of the blend without increasing the temperature.

Morphological Properties

The morphology in polymer blends is crucial for its thermal and mechanical properties. The morphologies of PBS/PEB blends obtained by SEM are depicted in Fig. 4. PBS showed a rough surface with a ductile behavior. The addition of PEB at different percentages led to variations in the morphology of the blends. In PBS95/PEB5, it was difficult to distinguish the phases preserving the morphology of PBS. Conversely, a distinct two-phase morphology was evident in PBS90/PEB10, wherein discrete droplets of the minor phase were dispersed within the matrix. The dispersion was homogeneous with PEB droplets ranging from 5 to 25 μm. However, some cavities were visible, derived from the debonding between the polymer phases during the cryogenic fracture [34]. Complete detachment indicated immiscibility and poor adhesion between the components in the blends. It becomes evident that, as the concentration increased, the minor PEB phase began to coalesce, forming larger droplets and cavities. This behavior was especially noticeable in PBS70/PEB30, where PEB domains reached 92 μm, representing a threefold increase compared to the
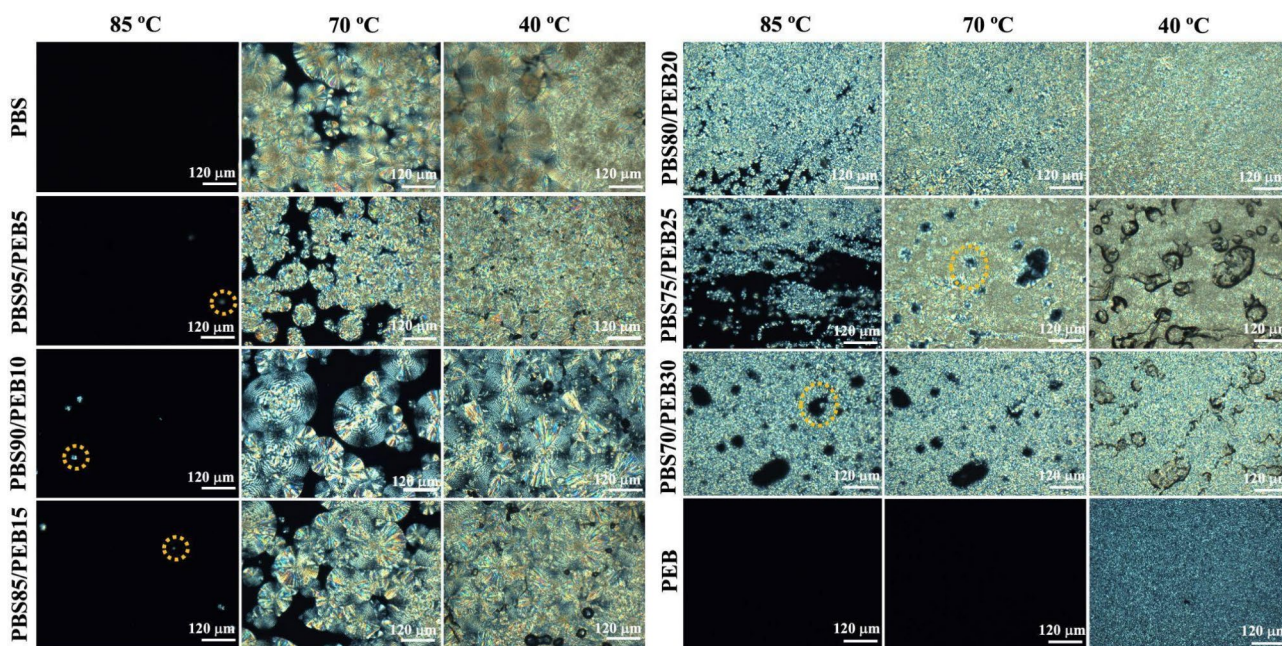
Fig. 5 Polarized optical micrographs of PBS, PEB, and PBS/PEB blends

other blends. PHB/PBSA blends have been reported to have an increase in the droplet size as the second component increases its proportion in the blend [17]. Wang et al. [35] attributed the increase in droplet size due to the differences in the melt viscosity and/or interfacial tension between components (polycaprolactone (PCL), isotactic poly(butene-1) PB, high-density polyethylene (HDPE) and polybutylene succinate (PBS). In general, PBS/PEB blends presented a sea-island morphology, in which PEB is dispersed in the continuous phase of PBS. Still, immiscibility between components was observed because of phase separation. The average size of the dispersed phase according to the composition was 7.05 μm, 12.08 μm, 15.62 μm, 30.27 μm, 33.80 μm and 35.45 μm for PBS95/PEB5, PBS90/PEB10, PBS85/PEB15, PBS80/PEB20, PBS75/PEB25, and PBS70/PEB30, respectively with significant differences between them ($p \leq 0.05$).

Polarized Optical: Crystal Behavior

Figure 5 depicts the polarized optical micrographs of PBS/PEB at various compositions and pure polymers after complete crystallization at 85 °C, 70 °C, and 40 °C. The neat PBS spherulites appeared after 80 °C and exhibited a well-developed radial growth pattern in their fibril structure. For pure PEB, fine spherulites were observed when cooling down to 40 °C, showing a faster crystallization rate and, therefore, a more significant nucleation density. The size of the spherulites of the pure PBS was 195.06 μm ± 45.7.

At 85 °C, the PBS80/PEB20 blend showed numerous small spherulites characterized by sizes and shapes that were notably smaller than those found in pure PBS. These findings revealed that PEB acted as a nucleating agent, accelerating the crystallization of PBS, as was observed in the increasing of T_c in PBS by DSC. Typically, a nucleating agent provides a surface that decreases the free energy barrier associated with the primary nucleation process. This, in turn, promoted an increase in nucleation density and a reduction of 92% in spherulite size showing an average of 16.14 μm ± 3.64.

In PBS/PEB blends in contrast with pure PBS and PEB, above a PEB content than 15%, from 85 °C was possible to observe a significant number of spherulites of PBS compared with pristine PBS; for this reason, the crystal density increased, the size diminished and the spherulites boundaries were not observed for PBS, indicating that below 20% of PEB, only PBS90/PEB10 and PBS85/PEB15 presented some spherulites but with much lower density at 85 °C. At lower temperatures, the number and size of PBS spherulites noticeably increased with an average value of 139.45 μm ± 29.14, and the shape was more irregular, like pristine PBS, but smaller than this.

Introducing a lower molecular weight polymer to PBS influenced the spherulite size, shape, and nucleation density. The variation of the crystal morphology of PBS caused by the addition of PEB is expected to affect the mechanical behavior of PBS and hence, the blend's performance.

X-ray Diffraction Pattern (XRD)

XRD diffraction patterns of PBS/PEB at different compositions are depicted in Fig. 6. Three strong peaks were observed for pure PBS at 2θ values of 19.6°, 22°, and 22.7° corresponding with the lattice parameters in the monoclinic unit cell (020), (021), and (110), respectively. In addition, PBS presented three weak peaks at 2θ = 26°, 29°, and 34° related to (-121), (111), and (121) planes. For neat PEB, the pattern showed three main diffraction peaks at 2θ = 21.5°, 24°, and 30°, which can be indexed as (110), (002), and (012), and a small peak at 2θ = 36° corresponding to (020) [36]. PBS/PEB diffraction pattern shows that the intensity of PBS peaks was reduced as PEB content increased, but it was more noticeable in the 2θ position 22.7°. For PEB, the behavior was similar depending on the content in the blend and more perceptible at 21.5°. In the blends, there are no observable new peaks, or significant peak shifts. This suggests that co-crystallization is unlikely to take place between the two polymers [37]. Instead, each component crystallizes independently, resulting in a phase separation.

The crystalline fraction for PEB was higher than PBS because of its lower molecular weight and easier chain mobility. In PBS/PEB blends, PEB acted as nucleating sites for PBS because it contributed to a higher percentage of crystallinity (see Table 2). For example, the highest value was found in the blend PBS95/PEB5, followed by PBS90/PEB10. However, as the PEB content increases above 15% in the blends, the percentage of crystallinity remains the same. All the blends showed values between PBS and PEB, with the closest values to PBS. In LLDPE/PBAT and LLDPE/PBS blends, the intensity of some peaks changed depending on the concentration of PBAT or PBS explained because of the variation in spherulite or crystal morphology, distribution, and the dispersion of the components. In PBAT/PBS, PBS content reduced the crystallinity of PBAT, and the addition of 40% and 60% of PBAT increased the
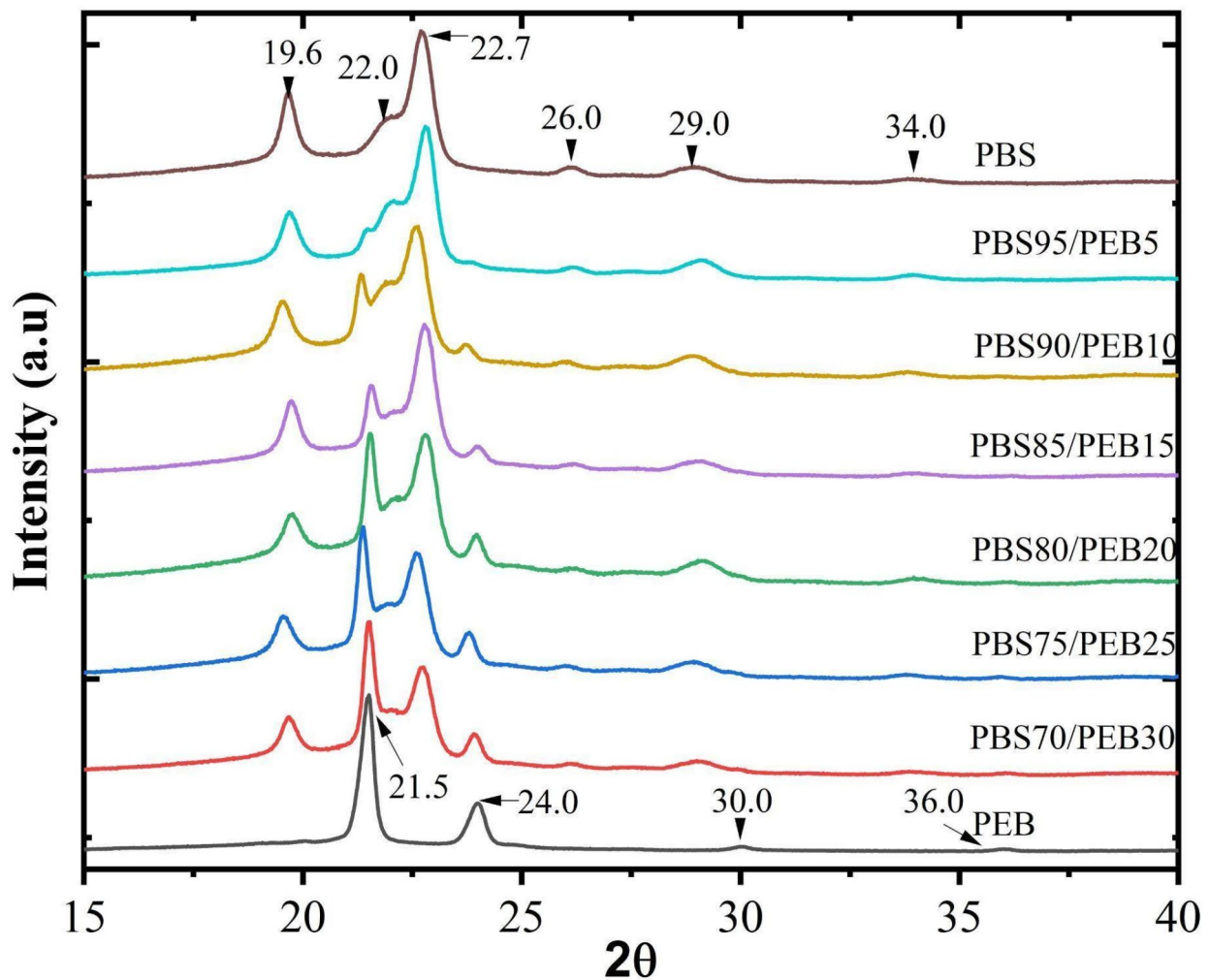

Fig. 6 X-ray diffraction patterns of PBS, PEB, and PBS/PEB blends

crystallinity of PBS [35]. PEB is expected to strongly modify the crystallization behavior of PBS and, hence, other properties.

Thermal Properties

Since PBS/PEB is an immiscible system, each component is expected to display its different properties independently within the blend, including thermal characteristics. Figure 7a shows the thermograms of the non-isothermal crystallization of PBS/PEB blends and neat polymers. PBS displayed a broad crystallization peak ($T_{c, PBS}$) starting around 54 ºC, whereas PEB exhibited a sharp peak ($T_{c, PEB}$) at 52.1 ºC. Based on the literature, in an immiscible blend of two crystalline polymers, if the difference in their T_m is sufficiently large, upon cooling from the melt, the polymer with the higher T_m tends to crystallize first in contact with the melt of the second polymer regardless of whether it is the matrix or the dispersed phase [38]. Nucleation frequently occurs on external surfaces, and its occurrence can be heightened by the migration of impurities or heterogeneities between various phases in the blending process [39]. Thus, the PBS crystallized first upon contact with the PEB melt. The interface between the PBS and PEB could serve as a region of concentrated nucleation activity. This requires an interface that readily wets the crystallizable polymer, thereby inducing heterogeneous nucleation.

In addition, $T_{c, PBS}$ shifted to higher values around 80 °C for PBS95/PEB5 due to the small nucleation sites that were homogeneously distributed in the system. The displacement was smaller in concentrations of 5% PEB, and even though the molten PEB acted as a nucleation agent, many of these sites may have coalesced, decreasing the number of grown sites. The PEB crystallized further at lower temperatures and in contact with a rigid phase due to the semicrystalline nature at the second phase (similar to the crystallization that a polymer undergoes in contact with another high T_g polymer) [38]. The $T_{c, PEB}$ for the PBS/PEB blends shifted at lower temperatures concerning neat PEB, because of the hindrance of the PEB chains to fold into the crystal
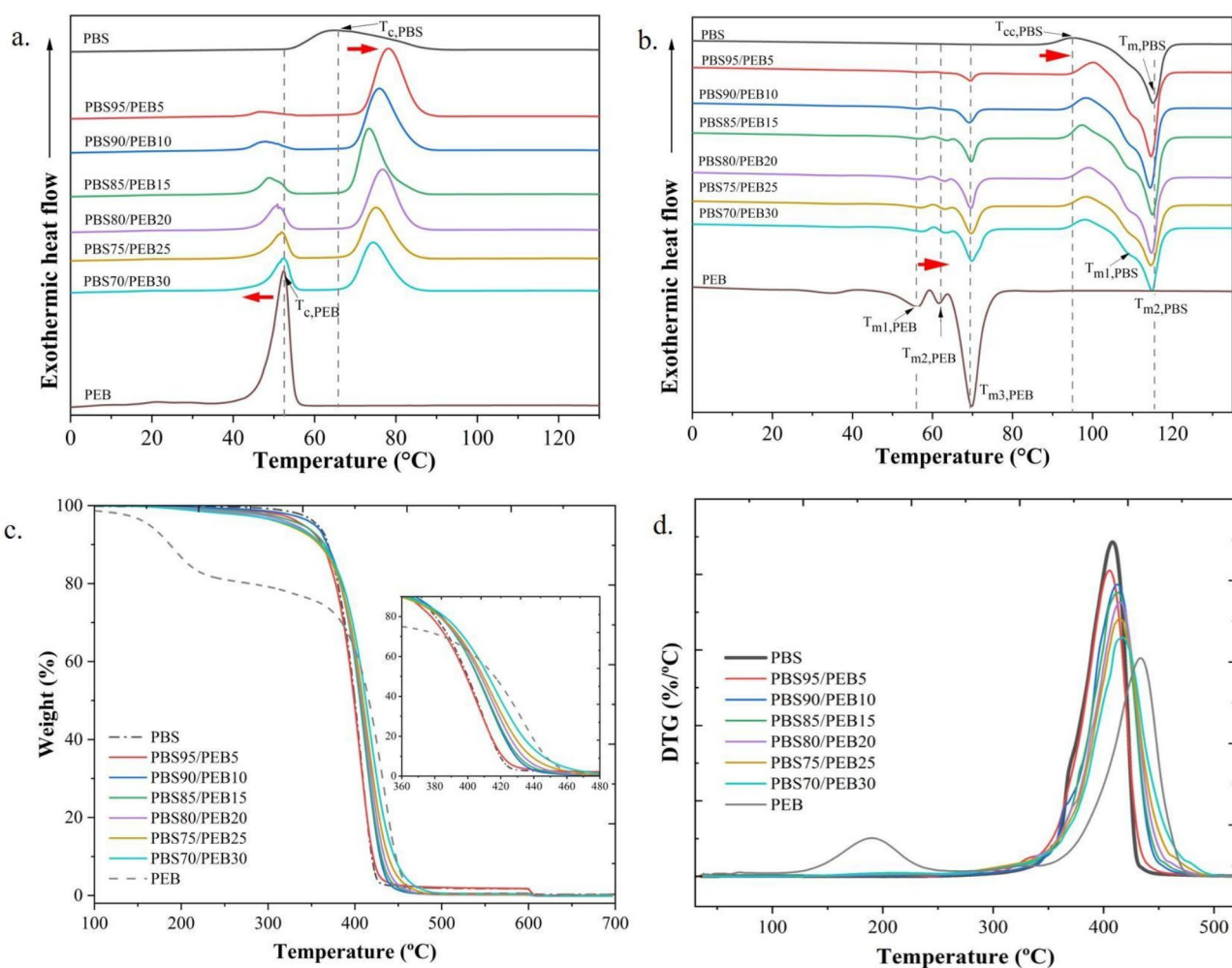

Fig. 7 DSC (a) cooling and (b) heating thermograms, (c) TGA curves and (d) DTG curves of PBS, PEB, and PBS/PEB blends

structure of the PBS. This behavior might also be associated with PEB droplets containing less efficient impurities that required higher solidification coolings, characteristic of the nucleating efficiency heterogeneity involved [40].

Figure 7b shows the heating process for the neat polymers and the corresponding blends. On the second heating, PBS displayed a broad peak ($T_{m, PBS}$) at 114 ºC and a small cold crystallization ($T_{cc, PBS}$) exotherm at around 95 ºC. According to Kajornprai et al. [41], the $T_{cc, PBS}$ is triggered by the simultaneous melt-recrystallization of the originally present PBS crystals, which have low thermal stability. Therefore, $T_{m, PBS}$ is derived from the melting of two distinct crystalline events: the recrystallized crystals formed during heating and those that initially existed in the PBS sample. Cold crystallization occurred because the PBS softens above its glass transition, which led to the polymer chains becoming more oriented [42]. Thus, further relaxation facilitated the alignment necessary for crystal growth.

In case of PEB, its melting peak splitted into three different peaks ($T_{m, PEB}$), suggesting a heterogeneous population of crystals of varying quality, which was typical of low molar mass PEB [11]. Previous studies have shown that cooling the system with ramps above 5 ºC/min promotes the formation of two (or more) types of crystals [43]. In our case, PEB presented three melting peaks derived from two crystal populations: the first peak around 56 °C produced by the melting of low thermal stability PEB crystals, a second peak at 62 °C caused to the simultaneous melting and recrystallization of high thermal stability PEB crystals, and the third peak at about 69 °C is derived by the melting of PEB crystals formed through the previously melt-recrystallized PEB crystals. The low molecular weight of PEB (Mw = 18, 400 Da) led to a very heterogeneous population with crystals of different thicknesses. T_g was not noticeable in the thermograms, possibly due to the high crystallinity of the polymer. Regarding PBS/PEB blends, two melting peaks were noticeable in all the compositions, denoting a semi-crystalline/semi-crystalline blend. The first peak ($T_{m, PEB}$) did not change with the PEB contents; probably, the melting points of the lamellae formed through the melt-recrystallization process matched that of the original lamellae during the second heating run. The second peak splitted into two new peaks ($T_{m1, PBS}$ and $T_{m2, PBS}$) that might be associated with a melting-recrystallization-melting event. The lowest temperature peak (T_{m1}) is attributed to the melting of the original crystal, while the highest (T_{m2}) refers to the melting of recrystallized crystals [21, 44]. It is worth mentioning that the presence of PEB delayed the cold crystallization of PBS which suggests that sufficiently stable nuclei were not formed due the presence of small amounts of amorphous and immiscible PEB segments [45].

As shown in Table 2, the ΔHc of PEB decreased monotonically compared to pure PEB as its concentration in the blend was reduced because PBS whose Xc is lower, inhibited its crystallization. The addition of PEB increased the degree of crystallinity in all the blends compared to pure PBS. This confirms that PEB acted as a plasticizer, allowing the PBS chains to move more easily. Thus, PEB promoted the chains' diffusion and packing, leading to crystal formation. Also, the addition of PEB gave rise to a higher ΔHc in PBS, demonstrating that PEB not only increased the Tc of PBS but also improved its degree of crystallinity. For other polymer blends, it was reported that plasticizers contribute to enhancing the crystallinity of a polymer, as in the case of PLA/PBS blends, where PBS acted as a plasticizer, increasing PLA bulk crystallinity [46]. A similar effect occurred in PBS/starch blends when an ionic liquid was added as a plasticizer [21]. The increase in the Xc of PBS further confirms the immiscibility between PBS and PEB. It is worth mentioning that the degree of crystallinity and crystalline pattern depend on the processing conditions in a similar way to any semicrystalline polymer. Xc values obtained by DSC ($X_{C2, DSC}$) during second heating differed from those obtained by XRD ($X_{C, XRD}$). This is attributed to the fact that XRD samples were not subjected to a controlled heat treatment that could promote the formation of better quality crystals. In addition, calculating PBS crystallinity from DSC traces requires an accurate measurement of the enthalpy of melting of 100% crystalline PBS. Unfortunately, the data available in the literature are widely dispersed ranging from 110 to 230 J g-1, so that it is unlikely to obtain similar values for $X_{C, DSC}$ and $X_{C, XRD}$. In both cases the same trend is maintained (See supplementary information, Table 4 S, Fig. 6S) The effect of adding PEB on the thermal degradation of PBS/PEB blends was analyzed. Figure 7c and d show the TGA and DTG curves. PBS showed one-step weight loss at 407.68 °C. PEB had two-step weight loss; the first was found at temperatures below 190.0 °C related to the evaporation of solvents used during PEB synthesis and some residual monomers, and then a principal weight loss at 434.16 °C. The higher maximum degradation temperature of PEB suggests a chemical structure that is more stable for thermal decomposition than PBS. Two weight losses were found for PBS/PEB blends: one due to PEB's first thermal decomposition and the other between PBS and PEB thermal decomposition. The maximum decomposition temperature for PBS95/PEB5 was 405.92 °C while PBS70/PEB30 was 417.25 °C (Fig. 7d). It was observed that the thermal stability under nitrogen atmosphere above 400 °C improved as PEB content increased.

T_c = crystallization temperature; ΔH_c = crystallization enthalpy; T_m = melting temperature; ΔH_m = melting enthalpy; T_{cc} = cold crystallization temperature; ΔH_{cc} =
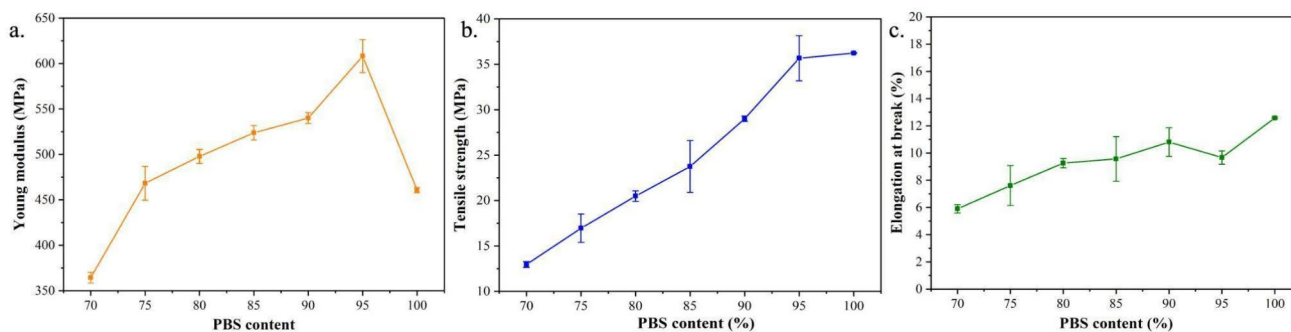
Fig. 8 Tensile properties of PBS and PBS/PEB blends

cold crystallization enthalpy. Different lowercase letters in the same column indicate a significant difference ($p \leq 0.05$).

Mechanical Performance

Stress-strain tests evaluated the mechanical properties of neat PBS and its blends with PEB. Figure 8 gives the mean values and dispersion of Young's modulus, tensile strength, and elongation at the break of PBS/PEB blends as a function of PBS content. Neat PBS used in this work was an injection molding grade with a high melt flow rate (MFR = 22 g/10 min) value, and it is a brittle material with a low percentage of elongation at break (< 25%). Biodegradable polyesters like PLA and PBS are characterized by their low elongation at break and brittleness [6]. The average values of the mechanical properties obtained with neat PBS agree with those reported in the literature by Dönitz et al. [47] and Rafiqah et al. [4].

Compared to neat PBS, the PBS/PEB blends increased their toughness; that is, Young's modulus increased (up to 608 MPa), but the tensile strength (from 36 MPa to 13 MPa) and the elongation at break (from 10 to 6%) decreased. These results agree with the morphology observed by polarized light optical microscopy (see Fig. 5). Incorporating PEB in higher contents increased the number of nuclei, giving rise to a greater density of crystals and spherulites with smaller sizes, making the material more brittle and hence the tensile strength and elongation at break diminished. A nucleating agent increases crystallinity; therefore, the modulus increases, the material becomes more rigid and brittle, and the tensile strength and elongation at break decreases. Then, increasing the PEB content, the blends gradually decreased all their mechanical properties owing to the low average molecular weight of PEB. The decrease in mechanical properties observed in blends with a higher content of PEB is related to the immiscibility of PEB in PBS and the poor adhesion between the phases (see Fig. 4).

Conclusions

The first proposal for PBS/PEB blending by melting was presented. The melt viscosity decreased, and a greater shear thinning behavior was observed with increasing PEB content, suggesting its lubricant effect favoring the motion of PBS chains. Incorporating PEB above 10 wt% led to variations in the rheological characteristics of the blends, attributed to the deformation of the dispersed phases. The morphology analysis revealed a well-dispersed PEB phase, but it was noticeable the formation of droplets that increased in size with higher PEB contents. This droplet enlargement indicates immiscibility and poor adhesion between components, and that each phase crystallized independently. PEB accelerates the crystallization of PBS due to heterogeneous nucleation, where the interface between PBS and PEB can act as a region of concentrated nucleation activity. PEB performs as a plasticizer or lubricant, allowing the PBS chains to move more easily; hence, PEB promotes the diffusion and packing of the PBS chains that lead to more numerous spherulites, homogeneous and smaller crystals.

The addition of PEB influenced the crystallization behavior of the PBS, consequently affecting its mechanical properties. The PBS95/PEB5 and PBS90/PEB10 blends presented an increase in tensile strength and Young's modulus, along with a decrease of shear viscosity of 34 and 60%, respectively, all without increasing the temperature. This suggests that these blends might achieve a favorable equilibrium between processability and mechanical performance in components produced through injection molding due to a faster crystallization and a lower viscosity.

Science Project A1-S-34241.

Declarations

References

1. Aversa C, Barletta M, Cappiello G, Gisario A (2022) Compatibilization strategies and analysis of morphological features of poly(butylene adipate-co-terephthalate) (PBAT)/poly(lactic acid) PLA blends: a state-of-art review. Eur Polym J 173:111304. https://doi.org/10.1016/J.EURPOLYMJ.2022.111304

2. Barletta M, Aversa C, Ayyoob M et al (2022) Poly(butylene succinate) (PBS): materials, processing, and industrial applications. Prog Polym Sci 132:101579. https://doi.org/10.1016/J.PROGPOLYMSCI.2022.101579

3. Thomas S, Grohens Y, Jyotishkumar P (2015) Characterization of Polymer blends: Miscibility, morphology and interfaces. Wiley Blackwell

4. Rafiqah SA, Khalina A, Harmaen AS et al (2021) A review on properties and application of bio-based poly(Butylene succinate). Polym (Basel) 13:1–28. https://doi.org/10.3390/polym13091436

5. Platnieks O, Gaidukovs S, Kumar Thakur V et al (2021) Bio-based poly (butylene succinate): recent progress, challenges and future opportunities. Eur Polym J 161:110855. https://doi.org/10.1016/J.EURPOLYMJ.2021.110855

6. Chang FL, Hu B, Huang WT et al (2022) Improvement of rheology and mechanical properties of PLA/PBS blends by in-situ UV-induced reactive extrusion. Polym (Guildf) 259:125336. https://doi.org/10.1016/J.POLYMER.2022.125336

7. Sabalina A, Gaidukovs S, Jurinovs M et al (2023) Fabrication of poly(lactic acid), poly(butylene succinate), and poly(hydroxybutyrate) bio-based and biodegradable blends for application in fused filament fabrication-based 3D printing. J Appl Polym Sci 140:1–13. https://doi.org/10.1002/app.54031

8. Chuakhao S, Rodríguez JT, Lapnonkawow S et al (2024) Formulating PBS/PLA/PBAT blends for biodegradable, compostable packaging: the crucial roles of PBS content and reactive extrusion. Polym Test 132:108383. https://doi.org/10.1016/j.polymertesting.2024.108383

9. Safari M, Pérez-Camargo RA, Ballester-Bayarri L et al (2022) Biodegradable binary blends of poly (butylene succinate) or poly (ε-caprolactone) with poly (butylene succinate-ran-ε-caprolactone)copolymers: crystallization behavior. Polym (Guildf) 256. https://doi.org/10.1016/j.polymer.2022.125206

10. Beluci N, de CL, Santos J dos, de Carvalho FA, Yamashita F (2023) Reactive biodegradable extruded blends of thermoplastic starch and polyesters. Carbohydr Polym Technol Appl 5:100274. https://doi.org/10.1016/j.carpta.2022.100274

11. Fernández J, Amestoy H, Sardon H et al (2016) Effect of molecular weight on the physical properties of poly(ethylene brassylate) homopolymers. J Mech Behav Biomed Mater 64:209–219. https://doi.org/10.1016/j.jmbbm.2016.07.031

12. Fernández J, Montero M, Etxeberria A, Sarasua JR (2017) Ethylene brassylate: searching for new comonomers that enhance the ductility and biodegradability of polylactides. Polym Degrad Stab 137:23–34. https://doi.org/10.1016/J.POLYMDEGRADSTAB.2017.01.001

13. Butron A, Llorente O, Fernandez J et al (2019) Morphology and mechanical properties of poly(ethylene brassylate)/cellulose nanocrystal composites. Carbohydr Polym 221:137–145. https://doi.org/10.1016/J.CARBPOL.2019.05.091

14. Budtri N, Aekrum S, Lertsiriyothin W (2017) The compatibility of polylactides and polybutylene succinate in PLA blends based on thermal, mechanical, and rheological properties. Orient J Chem 33:2766–2775. https://doi.org/10.13005/OJC/330609

15. Barletta M, Puopolo M (2020) Thermoforming of compostable PLA/PBS blends reinforced with highly hygroscopic calcium carbonate. J Manuf Process 56:1185–1192. https://doi.org/10.1016/J.JMAPRO.2020.06.008

16. Hirsch P, Menzel M, Klehm J, Putsch P (2019) Direct compounding injection molding and resulting properties of Ternary blends of Polylactide, Polybutylene Succinate and Hydrogenated Styrene Farnesene Block Copolymers. Macromol Symp 384:1800167. https://doi.org/10.1002/MASY.201800167

17. Righetti MC, Cinelli P, Aliotta L et al (2022) Immiscible PHB/PBS and PHB/PBSA blends: morphology, phase composition and modelling of elastic modulus. Polym Int 71:47–56. https://doi.org/10.1002/PI.6282

18. Lin C, Liu L, Liu Y, Leng J (2022) 4D printing of shape memory polybutylene succinate/polylactic acid (PBS/PLA) and its potential applications. Compos Struct 279:114729. https://doi.org/10.1016/j.compstruct.2021.114729

19. Abudula T, Saeed U, Memic A et al (2019) Electrospun cellulose Nano fibril reinforced PLA/PBS composite scaffold for vascular tissue engineering. J Polym Res 26. https://doi.org/10.1007/s10965-019-1772-y

20. Peshne H, Das KP, Sharma D, Satapathy BK (2024) Physicomechanical evaluation of Electrospun Nanofibrous Mats of Poly(3-hydroxybutyrate)/Poly(butylene succinate) blends with enhanced Swelling-Dynamics and Hydrolytic Degradation-kinetics Stability for Pliable Scaffold substrates. J Polym Environ. https://doi.org/10.1007/s10924-023-03174-5

21. Liu D, Qi Z, Zhang Y et al (2015) Poly(butylene succinate) (PBS)/ionic liquid plasticized starch blends: Preparation, characterization, and properties. Starch - Stärke 67:802–809. https://doi.org/10.1002/STAR.201500060

22. Boonprasertpoh A, Pentrakoon D, Junkasem J (2017) Investigating rheological, morphological and mechanical properties of PBS/PBAT blends. J Met Mater Min 27:1–11. https://doi.org/10.14456/jmmm.2017.1

23. Bhatia A, Gupta RK, Bhattacharya SN, Choi HJ (2009) An investigation of melt rheology and thermal stability of poly(lactic acid)/ poly(butylene succinate) nanocomposites. J Appl Polym Sci 114:2837–2847. https://doi.org/10.1002/APP.30933

24. Li R, Xu S, Xu J et al (2023) Effect of Functionalized Polyethylene Wax on the Melt Processing and properties of highly filled Magnesium Hydroxide/Linear Low-Density Polyethylene composites. Polym (Basel) 15:2575. https://doi.org/10.3390/POLYM15112575

25. Cross MM (1965) Rheology of non-newtonian fluids: a new flow equation for pseudoplastic systems. J Colloid Sci 20:417–437. https://doi.org/10.1016/0095-8522(65)90022-X

26. Lomellini P (1992) Williams-Landel-Ferry versus Arrhenius behaviour: polystyrene melt viscoelasticity revised. Polym (Guildf) 33:4983–4989. https://doi.org/10.1016/0032-3861(92)90049-3

27. Osswald TA, Rudolph NS (2015) Polymer rheology: fundamentals and applications, first edition. Hanser

28. Kalogeras IM, Brostow W (2009) Glass transition temperatures in binary polymer blends. J Polym Sci Part B Polym Phys 47:80–95. https://doi.org/10.1002/POLB.21616

29. Dealy JM, Wissbrun KF (1990) Melt rheology and its role in plastics processing, First edition. Springer US

30. Gui ZY, Wang HR, Gao Y et al (2012) Morphology and melt rheology of biodegradable poly(lactic acid)/poly(butylene succinate adipate) blends: effect of blend compositions. Iran Polym J (English Ed 21:81–89. https://doi.org/10.1007/S13726-011-0009-7/METRICS

31. Walha F, Lamnawar K, Maazouz A, Jaziri M (2016) Rheological, morphological and mechanical studies of sustainably sourced polymer blends based on poly(lactic acid) and polyamide 11. Polym (Basel) 8. https://doi.org/10.3390/polym8030061

32. Shaw MT (2011) Introduction to Polymer Rheology, First edition. John Wiley and Sons

33. Han CD (2007) Rheology and Processing of Polymeric materials: volume 1: Polymer Rheology. Oxford University Press

34. Fenni SE, Wang J, Haddaoui N et al (2019) Crystallization and self-nucleation of PLA, PBS and PCL in their immiscible binary and ternary blends. Thermochim Acta 677:117–130. https://doi.org/10.1016/J.TCA.2019.03.015

35. Bumbudsanpharoke N, Wongphan P, Promhuad K et al (2022) Morphology and permeability of bio-based poly(butylene adipate-co-terephthalate) (PBAT), poly(butylene succinate) (PBS) and linear low-density polyethylene (LLDPE) blend films control shelf-life of packaged bread. Food Control 132. https://doi.org/10.1016/j.foodcont.2021.108541

36. Xu Y, Xu J, Liu D et al (2008) Synthesis and characterization of biodegradable poly(butylene succinate-co-propylene succinate) s. J Appl Polym Sci 109:1881–1889. https://doi.org/10.1002/APP.24544

37. Zhang X, Liu Q, Shi J et al (2018) Distinctive Tensile properties of the blends of poly(l-lactic acid) (PLLA) and poly(butylene succinate) (PBS). J Polym Environ 26:1737–1744. https://doi.org/10.1007/S10924-017-1064-8/METRICS

38. Tien ND, Prud'homme RE (2018) Crystallization behavior of Semicrystalline Immiscible Polymer blends. In: Thomas S, Arif P M, Bhoje Gowd E, Kalarikkal N (eds) Crystallization in Multiphase Polymer systems. Elsevier, pp 181–212. https://doi.org/10.1016/B978-0-12-809453-2.00007-4

39. Fenni SE, Cavallo D, Müller AJ (2019) Nucleation and crystallization in Bio-based Immiscible Polyester blends. In: Di Lorenzo ML, Androsh R (eds) Thermal properties of bio-based polymers. Springer Science and Business Media Deutschland GmbH, pp 219–256

40. Wang B, Utzeri R, Castellano M et al (2020) Heterogeneous nucleation and self-nucleation of Isotactic Polypropylene microdroplets in Immiscible blends: from nucleation to growth-dominated crystallization. Macromolecules 53:5980–5991

41. Kajornprai T, Sirisinha K (2021) Effect of thermal annealing on crystal evolution and multiple melting behaviors of molded poly(L-lactic acid) and poly(butylene succinate) blends upon heating investigated by TMDSC. J Therm Anal Calorim 146:2471–2480. https://doi.org/10.1007/S10973-021-10629-1

42. Ishino K, Shingai H, Hikita Y et al (2021) Cold crystallization and the Molecular structure of Imidazolium-based ionic liquid crystals with a p-Nitroazobenzene Moiety. ACS Omega 6:32869–32878. https://doi.org/10.1021/ACSOMEGA.1C04866/SUPPL_FILE/AO1C04866_SI_004.PDF

43. Marxsen SF, Song D, Zhang X et al (2022) Crystallization rate Minima of Poly(ethylene brassylate) at temperatures transitioning between Quantized Crystal thicknesses. Macromolecules. https://doi.org/10.1021/ACS.MACROMOL.2C00308/ASSET/IMAGES/LARGE/MA2C00308_0012.JPEG

44. Ye HM, Tang YR, Xu J, Guo BH (2013) Role of poly(butylene fumarate) on crystallization behavior of poly(butylene succinate). Ind Eng Chem Res 52:10682–10689

45. Wellen RMR, Canedo EL (2014) On the Kissinger equation and the estimate of activation energies for non-isothermal cold crystallization of PET. Polym Test 40:33–38. https://doi.org/10.1016/J.POLYMERTESTING.2014.08.008

46. Park JW, Im SS (2002) Phase behavior and morphology in blends of poly(L-lactic acid) and poly(butylene succinate). J Appl Polym Sci 86:647–655. https://doi.org/10.1002/APP.10923

47. Dönitz A, Köllner A, Richter T et al (2023) Additive Manufacturing of Biodegradable Hemp-Reinforced Polybutylene Succinate (PBS) and its mechanical characterization. Polym (Basel) 15:1–18. https://doi.org/10.3390/polym15102271